mathematics

IMPACT FACTOR 2.4

CITESCORE 3.5

Article

Thermal Responses and the Energy Spectral of Diatomic Molecules Using Nikiforov–Uvarov Methodology

Muhammad Roshanzamir

MDPI

https://doi.org/10.3390/math11153338

mathematics

MDPI

Article

Thermal Responses and the Energy Spectral of Diatomic Molecules Using Nikiforov–Uvarov Methodology

Muhammad Roshanzamir

Division of Elementary Particles and Field Theory, Department of Physics, Faculty of Basic Sciences, Shahrekord University, Shahrekord 64165478, Iran; m.roshanzamir@sku.ac.ir

Abstract: The parametric Nikiforov–Uvarov approach and the Greene–Aldrich approximation scheme were used to achieve approximate analytical solutions to the Schrödinger equation, involving an interaction of the modified deformed Hylleraas potential mixed linearly with the improved Frost–Musulin diatomic molecular potential. For each ℓ-state, the energy spectra and normalized wave functions were generated from the hypergeometric function in the closed form. The thermal properties of such a system, including the vibrational partition function, vibrational mean energy, vibrational mean free energy, vibrational specific heat capacity, and vibrational entropy, were then calculated for the selected diatomic molecules using their experimental spectroscopic parameters. Furthermore, the peculiar conditions of this potential were evaluated, and their energy eigenvalues were calculated for the purpose of comparison. The acquired results were found to be in reasonable agreement with those reported in the literature.

Keywords: thermal properties; Greene–Aldrich approximation; energy spectra; Schrödinger equation

MSC: 81V55; 81Q05; 34L16

Citation: Roshanzamir, M. Thermal Responses and the Energy Spectral of Diatomic Molecules Using Nikiforov–Uvarov Methodology. *Mathematics* **2023**, *11*, 3338. https://doi.org/10.3390/math11153338

Academic Editor: Stoytcho Stoyanov Yazadjiev

Received: 20 March 2023
Revised: 28 April 2023
Accepted: 4 May 2023
Published: 30 July 2023

1. Introduction

In recent years, several studies have focused on the examination of quantum mechanical concerns with diverse physical potentials because they include all of the necessary features required to appropriately define physical quantum models [1–3]. Describing the Schrödinger wave equation for particles interacted via the physical potential terms of interest in quantum mechanics has prompted substantially more thought in several researchers, as well as its significant influence on quantum mechanics in diverse areas of physics and chemistry [4,5]. It leads to a precise explanation of the particles' behavior in quantum mechanics and may serve as a prologue to the examination of other features such as thermodynamics [6,7], mass spectra of quarkonia systems [8–10], and the structure of diatomic molecules [11–14].

It is also recognized that the explicit viable actual possibilities through the Schrödinger equations are uncommon, with the exception of several notable solvable quantum systems, such as the hydrogen atom [15] and harmonic oscillator [16,17], whereas the case of states with arbitrary angular momentum, which do not reveal exact solutions, is known analytically or by approximation methods [18,19]. These solutions have vital uses in many domains of physics and chemistry for assessing and enhancing the models established to analyze quantum mechanical systems, as well as for developing numerical approaches. As a consequence, several quantum modes should indeed be treated through approximation schemes if the solutions of the wave equation are to be obtained under such a system; the choice of these applicable approximation layouts is based on their adaptability to the required potential [20,21]. Because of their diverse uses, solutions to the relativistic and non-relativistic wave equations have been used in various quantum potential interactions employing various methodologies [22,23]. These approaches include the 1/N

shifted expansion procedure [24], the Nikiforov–Uvarov approach [25–27], the asymptotic iteration method [28], the factorization method [29,30], the formula technique [31], the supersymmetric approach [32,33], the ansatz methodology [34], the Laplace transform approach [35,36], the functional analysis approach [37,38], the appropriate quantization rule [39], and others [40,41]. For many solvable quantum frameworks, the hypergeometric Nikiforov–Uvarov technique has demonstrated its ability to determine the exact energy levels of bound states [42]. The parametric adaptation of this method is used in this study to obtain the bound state solutions of the radial Schrödinger equation. Its satisfactory execution is backed by comparisons with numerous methodologies as well as a straightforward, precise, and user-friendly approach.

Various quantum mechanical wave equations have been widely explored using exponential-type potentials [43,44]. It is argued that these potentials are far more efficient than their counterparts, which exist in Coulomb or inverse forms [45] and play important roles in solid-state physics, nuclear physics, and other intriguing fields [46,47]. An appropriate form of a composite exponential-type potential is assumed in the study of potentials with hypergeometric wavefunctions, allowing for the generation of varied exponential potentials and a broader variety of applications. Such potentials may be extensively used as interaction models of diatomic molecules, which motivated the current investigation. The desired combined potential encompasses the modified deformed Hylleraas potential with an improved Frost–Musulin diatomic molecular potential function, which is given by

$$V(r) = D_e\left(1 - \frac{\left(r + \sigma r_e r - \sigma {r_e}^2\right)e^{-\sigma(r-r_e)}}{r}\right) - \frac{e^{-\sigma r}}{1-e^{-\sigma r}}\left(-\frac{V_0}{b}(ae^{\sigma r}-1) + V_1 - \frac{V_2}{1-e^{-\sigma r}}\right) \tag{1}$$

where D_e, σ and r_e are the dissociation energy, the screening parameter, and the equilibrium bond length, respectively, where $\sigma < 1$ and V_0, V_1 and V_2 are the depths of the potential well, and a along with b are two adjustable parameters representing the properties of the potential. Because it includes the significant potential models as special instances, this combination might reflect the effective potential of a many-body system, Figure 1. This paradigm may be applied to atomic, solid-state, plasma, and molecular physics. As a result, in some circumstances, this potential provides superior therapy to other exponential potentials and has the ability to affect the efficiency of other potentials. As a result, the investigation of quantum systems associated with these types of potentials appears to be significant in suggesting numerous frameworks for quantum chemistry and molecular physics. Despite the fact that there has been little research into this linear combination of diatomic molecule potential energy functions, the current inquiry was driven by the concept that this form of potential might be used as a mathematical example to strikingly illustrate intramolecular and intermolecular interactions and atomic pair correlations, as well as to check the accuracy of the models and approximations in computational physics and chemistry as well as in quantum mechanics. As a result, the success of quantum mechanics in depicting the physics of atomic and subatomic particles cannot be emphasized [22,46,48,49].

Various differential problems may be solved using the Nikiforov–Uvarov technique in mathematical physics, which is founded on masking a second-order linear differential equation to an extended equation of a hypergeometric type [25]. Several breakthroughs in utilizing this methodology to successfully generate genuine solutions for different wave equations in a quantum system have been described [50,51]. This technique's parametric form was designed to have a practical deployment [27] and can effectively solve certain systems of equations of type

$$\left(\frac{d^2}{ds^2} + \frac{\wp_1 - \wp_2 s}{s(1-\wp_3 s)}\frac{d}{ds} - \frac{1}{(s(1-\wp_3 s))^2}\left(\mathcal{E}_1 s^2 - \mathcal{E}_2 s + \mathcal{E}_3\right)\right)\psi(s) = 0. \tag{2}$$

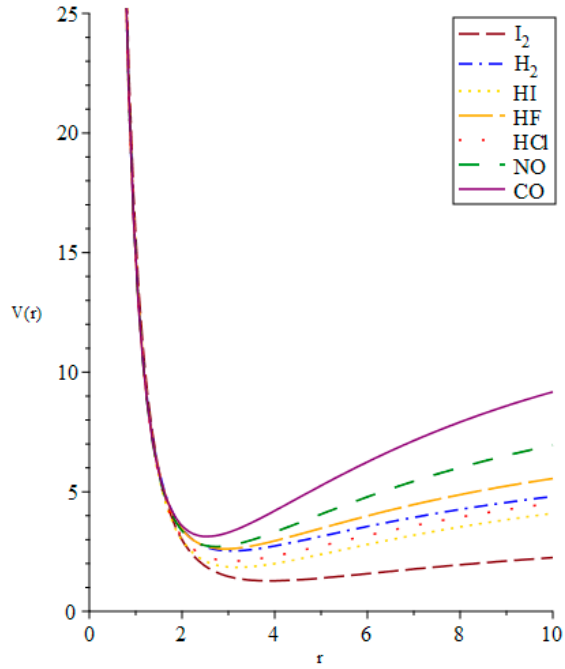

Figure 1. Sketch of the composed-potential as a function of r $(r > 0)$ with $(V_0, V_1, V_2, a, b) = (0.8, 0.4, 0.5, 0.6, 0.3)$ for $\sigma = 0.15$.

The eigenfunctions are represented as follows in this approach,

$$\psi(s) = \mathcal{N}_{n,\ell}\, s^{\wp_{12}}(1-\wp_3 s)^{-\wp_{12}-\frac{\wp_{13}}{\wp_3}}\, \mathcal{P}_n^{(\wp_{10}-1,\frac{\wp_{11}}{\wp_3}-\wp_{10}-1)}(1-2\wp_3 s) \tag{3}$$

where $\mathcal{P}_n^{(\alpha,\beta)}(x)$ and $\mathcal{N}_{n,\ell}$ are the orthogonal Jacobi polynomial [52] and the normalization constant, respectively. The following condition yields the parametric energy eigenvalues as

$$\begin{gathered}\wp_2 n-(2n+1)\wp_5+(2n+1)\left(\sqrt{\wp_9}+\wp_3\sqrt{\wp_8}\right)+n(n+1)\wp_3+2\wp_3\wp_8 \\ +2\sqrt{\wp_8\wp_9}+\wp_7=0,\end{gathered} \tag{4}$$

where

$$\begin{gathered}\wp_4=\tfrac{1}{2}(1-\wp_1), \wp_5=\tfrac{1}{2}(\wp_2-2\wp_3),\ \wp_6=\wp_5^2+\mathcal{E}_1,\ \wp_7=2\wp_4\wp_5-\mathcal{E}_2, \\ \wp_8=\wp_4^2+\mathcal{E}_3,\ \wp_9=\wp_3\wp_7+\wp_3^2\wp_8+\wp_6,\ \wp_{10}=\wp_1+2\wp_4+2\sqrt{\wp_8}, \\ \wp_{11}=\wp_2-2\wp_5+2\left(\sqrt{\wp_9}+\wp_3\sqrt{\wp_8}\right),\ \wp_{12}=\wp_4+\sqrt{\wp_8}, \\ \wp_{13}=\wp_5-\left(\sqrt{\wp_9}+\wp_3\sqrt{\wp_8}\right).\end{gathered} \tag{5}$$

In this sense, the requirements for this paper are as follows: Section 2 applies the fundamental notion of the parametric Nikiforov–Uvarov method via the Greene–Aldrich approximation technique to derive ℓ-wave approximate analytical solutions of the radial Schrödinger equation and the normalized radial wavefunctions in terms of the generalized hypergeometric functions for the appropriate potential. There is a great deal of interest in using various potential energy functions and experimentally established spectroscopic data to solve a variety of problems, including thermodynamic quantity calculations [53,54]. To the state of the art, the energy spectra and corresponding thermodynamic properties for the linear combination of the modified deformed Hylleraas potential with the improved Frost–Musulin diatomic molecular potential function have not been obtained, motivating the author to investigate the nonrelativistic vibrational energy and corresponding thermal responses of such a system within the Schrödinger equation in Section 3. Section 4 is devoted to a brief discussion, followed by a summary of the conclusions.

2. Any ℓ-State Solutions through the Greene–Aldrich Approximation and Parametric Nikiforov–Uvarov Approach

For an empirical potential, the radial Schrödinger equation is stated as [55]

$$\left(\frac{d^2}{dr^2}+\frac{2\mu}{\hbar^2}\left(E_{n,\ell}-V(r)-\frac{\ell(\ell+1)\hbar^2}{2\mu r^2}\right)\right)U_{n,\ell}(r)=0, \tag{6}$$

where $\hbar$, μ and $E_{n,\ell}$ are the reduced Planck's constant, the reduced mass of the particle, and the rotational-vibrational energy of the diatomic molecules, respectively. n and ℓ represent the radial and orbital angular momentum quantum numbers. This equation is a nonrelativistic wave equation for diatomic molecules with an effective potential specified as $V(r)+\ell(\ell+1)\hbar^2/2\mu r^2$ where the boundary condition of $U_{n,\ell}(r)$ vanishes at the points $r = 0$ and $r\to\infty$. Substituting Equation (1) into Equation (6) and rearranging, the following second-order Schrödinger equation may be acquired as

$$\begin{aligned}\left(\frac{d^2}{dr^2}+\frac{2\mu E_{n,\ell}}{\hbar^2}\right. & -\frac{2\mu}{\hbar^2}D_e-\frac{\ell(\ell+1)}{r^2}\\ & -\frac{2\mu}{\hbar^2}\frac{e^{-\sigma r}}{1-e^{-\sigma r}}\left(+\frac{V_0}{b}(ae^{\sigma r}-1)-V_1+\frac{V_2}{1-e^{-\sigma r}}\right)\\ & \left.+\frac{2\mu}{\hbar^2}D_e\frac{\left(r+\sigma r_e r-\sigma {r_e}^2\right)e^{-\sigma(r-r_e)}}{r}\right)U_{n,\ell}(r)=0,\end{aligned} \tag{7}$$

which cannot be solved analytically even in the s-wave case. The following Greene–Aldrich approximation approach might be utilized [19,56], for $\sigma \ll 1$ as

$$\frac{1}{r^2}\approx\frac{\sigma^2}{\left(1-e^{-\sigma r}\right)^2}, \tag{8}$$

to solve Equation (7) for any given ℓ-state while additionally considering the columbic characteristic $(1/r)$ of the suggested potential. Figure 2 compares the trend of $1/r^2$ with the proposed approximation term. This approximation appeared to be most appropriate for the low values of σ that were investigated in this research. As a result, this approximation was employed throughout this inquiry.

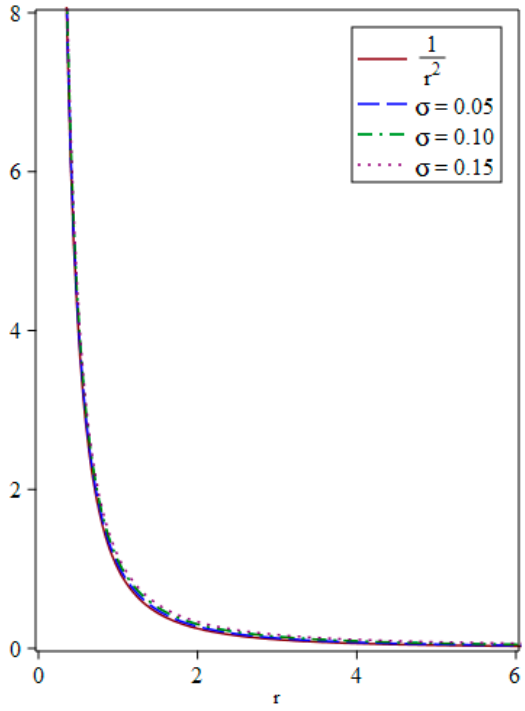

Figure 2. Plot of $\frac{1}{r^2}$ and its approximation in Equation (10) with $\sigma = 0.05,\ 0.10$ and 0.15.

By substituting Equation (8) into Equation (7) and applying the coordinate transformation of the form $\mathcal{P} = e^{-\sigma r}$, the modified hypergeometric-type equation was given as

$$\frac{d^2U_{n,\ell}(h)}{d\mathcal{P}^2} + \frac{1}{\mathcal{P}}\frac{dU_{n,\ell}(\mathcal{P})}{d\mathcal{P}} + \frac{1}{\mathcal{P}^2(1-\mathcal{P})^2}\Big(-\mathcal{E}_1\mathcal{P}^2 + \mathcal{E}_2\mathcal{P} - \mathcal{E}_3\Big)U_{n,\ell}(\mathcal{P}) = 0, \tag{9}$$

where

$$\mathcal{E}_1 = \frac{-2\mu}{\hbar^2\sigma^2}\left(D_e\sigma r_e e^{\sigma r_e}(r_e+1) + E_{n,\ell} + D_e(e^{\sigma r_e}-1) - \left(\frac{V_0}{b} - V_1\right)\right), \tag{10}$$

$$\mathcal{E}_2 = \frac{2\mu}{\hbar^2\sigma^2}\left(\frac{V_0}{b}(a+1) + V_1 - V_2 - D_e\sigma r_e e^{\sigma r_e}(r_e+2) - 2E_{n,\ell} - 2D_e(e^{\sigma r_e}-1)\right), \tag{11}$$

$$\mathcal{E}_3 = \frac{-2\mu}{\hbar^2\sigma^2}\left(E_{n,\ell} - D_e(1-e^{\sigma r_e}(\sigma r_e+1)) - \frac{aV_0}{b}\right) + \ell(\ell+1). \tag{12}$$

The corresponding parametric coefficients might well be derived by analogizing Equation (9) with Equation (2), as

$$\begin{aligned}\wp_1 = \wp_2 = \wp_3 = {} & 1,\ \wp_4 = 0,\ \wp_5 = -\tfrac{1}{2},\ \wp_6 = \tfrac{1}{4} + \mathcal{E}_1,\ \wp_7 = -\mathcal{E}_2,\ \wp_8 = \mathcal{E}_3,\ \wp_9 \\ & = \mathcal{E}_1 - \mathcal{E}_2 + \mathcal{E}_3 + \tfrac{1}{4},\ \wp_{10} = 1 + 2\sqrt{\mathcal{E}_3},\ \wp_{11} \\ & = 2\left(1 + \sqrt{\mathcal{E}_3} + \sqrt{\mathcal{E}_1 - \mathcal{E}_2 + \mathcal{E}_3 + \tfrac{1}{4}}\right),\ \wp_{12} = \sqrt{\mathcal{E}_3},\ \wp_{13} \\ & = -\tfrac{1}{2} - \sqrt{\mathcal{E}_3} - \sqrt{\mathcal{E}_1 - \mathcal{E}_2 + \mathcal{E}_3 + \tfrac{1}{4}}.\end{aligned} \tag{13}$$

By substituting Equation (13) into Equation (4), the relevant nonrelativistic energy spectra for the modified deformed Hylleraas potential coupled directly with the improved Frost–Musulin diatomic molecular potential model could be obtained precisely as

$$\begin{aligned}E_{n,\ell} = {} & \frac{1}{2\mu}\Bigg(\Bigg(-\frac{2D_e\mu(\sigma r+1)e^{\sigma r}}{\sigma^2\hbar^2} + \frac{2a\mu V_0}{\sigma^2\hbar^2 b} + \frac{2\mu D_e}{\sigma^2\hbar^2} + \ell(\ell+1) \\ & - \Bigg(\frac{-\frac{2D_e\mu r^2 e^{\sigma r}}{\sigma\hbar^2} - \frac{2(a-1)\mu V_0}{\sigma^2\hbar^2 b} + \frac{2\mu V_1}{\sigma^2\hbar^2} - \ell(\ell+1)}{2n+1+2\sqrt{\left(\ell+\frac{1}{2}\right)^2 + \frac{2\mu V_2}{\sigma^2\hbar^2}}} + \frac{n}{2} + \frac{1}{4} + \frac{\sqrt{\left(\ell+\frac{1}{2}\right)^2 + \frac{2\mu V_2}{\sigma^2\hbar^2}}}{2}\Bigg)^2\Bigg)\sigma^2\hbar^2\Bigg).\end{aligned} \tag{14}$$

Furthermore, by replacing Equation (13) with Equation (3), the appropriate wavefunction for the suggested potential was achieved,

$$U_n(\wp) = \mathcal{N}_n\wp^{\zeta}(1-\wp)^{\rho}\mathcal{P}_n^{(2\zeta,2\rho-1)}(1-2\wp), \tag{15}$$

where

$$\begin{aligned}\zeta &= \tfrac{1}{\hbar\sigma}\sqrt{2\mu\left(D_e(1-e^{\sigma r_e}(\sigma r_e+1)) - E_{n,\ell} + \tfrac{aV_0}{b}\right) + \ell(\ell+1)}, \\ \rho &= \tfrac{1}{2}\left(1 + \sqrt{\tfrac{4\sigma^2\left(\ell+\frac{1}{2}\right)^2\hbar^2 + 8\mu V_2}{\sigma^2\hbar^2}}\right),\end{aligned} \tag{16}$$

and $\mathcal{P}_n^{(\chi,\varsigma)}$ refers to the Jacobi polynomials, which are widely applied in mathematical analysis and practical applications. The orthogonality feature of these polynomials [52] may be used to represent the normalizing coefficient,

$$\begin{aligned}\int_{-1}^{1}\mathcal{P}_a^{(\chi,\varsigma)}\mathcal{P}_b^{(\chi,\varsigma)} & (1-t)^{\chi}(1+t)^{\varsigma}dt \\ & = \tfrac{2^{\chi+\varsigma+1}}{2n+\chi+\varsigma+1}\tfrac{\Gamma(n+\chi+1)\Gamma(n+\varsigma+1)}{n!\Gamma(n+\chi+\varsigma+1)}\delta_{ab}.\end{aligned} \tag{17}$$

In this manner, the normalization coefficient $\mathcal{N}_n$ can be expressed as

$$\mathcal{N}_n = \left(\frac{\zeta\sigma(\rho+n+\zeta)\Gamma(n+1)\Gamma(\rho+n+2\zeta-1)}{(n+\rho)\Gamma(n+2\rho)} \right)^{\frac{1}{2}}. \tag{18}$$

3. The Thermal Behaviour of the Schrödinger Equation with MDH-IFM Potential

Thermal properties are considered as characteristic features of a system capable of determining its state. To investigate the thermodynamic features of the proposed potential model in which only pure vibrational states were addressed, we recast Equation (14) in the form

$$E_{n,\ell} = \frac{\hbar^2\sigma^2}{2\mu}\left(T_1 - \left(\frac{T_2}{2(n+\eta)} + \frac{n+\eta}{2} \right)^2 \right), \tag{19}$$

where

$$\begin{gathered} T_1 = -2D_e\mu\tfrac{\sigma r+1}{\hbar^2\sigma^2}e^{\sigma r} + \tfrac{2a\mu V_0}{\hbar^2\sigma^2 b} + \tfrac{2\mu D_e}{\hbar^2\sigma^2} + \ell(\ell+1), \\ T_2 = \tfrac{-2D_e\mu r^2}{\hbar^2\sigma}e^{\sigma r} - \ell(\ell+1) - \tfrac{2\mu V_0(a-1)}{\hbar^2\sigma^2 b} + \tfrac{2\mu V_1}{\hbar^2\sigma^2}, \\ \eta = \tfrac{1}{2} + \sqrt{\left(\ell+\tfrac{1}{2}\right)^2 + \tfrac{2\mu V_2}{\hbar^2\sigma^2}},\ n = 0,1,2,\ldots < \left[-\eta + \sqrt{T_1} \pm \sqrt{T_1 - T_2}\ \right]. \end{gathered} \tag{20}$$

The primary objective for investigating a system's thermodynamic characteristics is to evaluate its vibrational partition function, which is commonly regarded as the cornerstone of statistical thermodynamics.

3.1. Partition Function

The calculation of thermodynamic functions [56], whose applications are frequently employed in statistical mechanics and molecular physics [55,57], is aided by the vibrational partition function for any given potential system. This intriguing function expressly relies on temperature and is commonly referred to as the Boltzmann distribution function in statistical mechanics, which was initially introduced by Boltzmann in 1870 [58]. For certain potential models, the partition function may be determined simply by adding all the possible rotational-vibrational energy levels to the system. The partition function $Q(\beta)$ of the modified deformed Hylleraas potential with the improved Frost–Musulin diatomic molecular potential at a finite temperature T may be calculated by using the energy spectra of Equation (19) as

$$Q_{vib}(\beta) = \sum_{n=0}^{\varpi} e^{-\beta E_{n,\ell}},\ \beta = \frac{1}{\kappa T},\ \varpi = -\eta + \sqrt{T_1} \pm \sqrt{T_1 - T_2}\,, \tag{21}$$

where $\beta = 1/\kappa T$ with κ is the Boltzmann constant. Hence,

$$\begin{aligned} Q_{vib}(\beta) = \tfrac{1}{2\sqrt{-\varkappa\mu\beta}} \quad & \left(\left(1 - \operatorname{erf}\left(\left(\tfrac{\sqrt{-\varkappa T_2{}^2}}{2(n+\eta)} - \tfrac{(n+\eta)\sqrt{-\varkappa}}{2} \right)\sqrt{\beta} \right) \right. \right. \\ & \left. \left. -e^{T_2\varkappa\beta}\left(1 - \operatorname{erf}\left(\left(\tfrac{\sqrt{-\varkappa T_2{}^2}}{2(n+\eta)} + \tfrac{(n+\eta)\sqrt{-\varkappa}}{2} \right)\sqrt{\beta} \right) \right) \right) \sqrt{\pi} e^{-T_1\beta\varkappa} \right). \end{aligned} \tag{22}$$

The error function (a normalized variant of the Gaussian function), commonly abbreviated as erf (w), is a comprehensive function defined as:

$$\operatorname{erf}(w) \equiv 2\pi^{-\frac{1}{2}} \int_0^w e^{-z^2} dz,$$

The various thermodynamic variables of the current system, such as vibrational mean energy, vibrational mean free energy, vibrational specific heat capacity, vibrational entropy, and others, may be easily determined from the canonical partition function as shown below.

3.2. The Vibrational Mean Energy

Evaluating the thermodynamic value of the total energy can also be used to illustrate the partition function's utility. The expected value, or ensemble average, for the energy is just the sum of the microstate energies weighted by their probabilities. The vibrational mean free energy of the modified deformed Hylleraas potential with improved Frost–Musulin diatomic molecular potential is calculated as follows:

$$\begin{aligned} U_{vib}(\beta) &= -\tfrac{\partial}{\partial\beta}\ln Q_{vib}(\beta) \\ &= \left(\left(\tfrac{1}{2}+\varkappa(T_1-T_2)\beta\right)\sqrt{\pi}e^{T_2\beta\varkappa}(n+\eta)\operatorname{erf}\left(\frac{\left(\sqrt{-{T_2}^2\varkappa}+\sqrt{-\varkappa}(n+\eta)^2\right)\sqrt{\beta}}{2(n+\eta)}\right)\right. \\ &\quad -\frac{\left(-\sqrt{-{T_2}^2\varkappa}+\sqrt{-\varkappa}(n+\eta)^2\right)\sqrt{\beta}e^{-\frac{\beta\left(-\sqrt{-{T_2}^2\varkappa}+\sqrt{-\varkappa}(n+\eta)^2\right)^2}{4(n+\eta)^2}}}{2} \\ &\quad -\frac{e^{T_2\beta\varkappa}\left(\sqrt{-{T_2}^2\varkappa}+\sqrt{-\varkappa}(n+\eta)^2\right)\sqrt{\beta}e^{-\frac{\beta\left(\sqrt{-{T_2}^2\varkappa}+\sqrt{-\varkappa}(n+\eta)^2\right)^2}{4(n+\eta)^2}}}{2} \\ &\quad +\sqrt{\pi}\left(\left(-\tfrac{1}{2}-\varkappa(T_1-T_2)\beta\right)e^{T_2\beta\varkappa}\right. \\ &\quad \left.\left.+\left(1+\operatorname{erf}\left(\frac{\left(-\sqrt{-{T_2}^2\varkappa}+\sqrt{-\varkappa}(n+\eta)^2\right)\sqrt{\beta}}{2(n+\eta)}\right)\right)\left(T_1\varkappa\beta+\tfrac{1}{2}\right)\right)(n+\eta)\right) \\ &\quad \times\left(\sqrt{\pi}\beta(n+\eta)\left(e^{T_2\beta\varkappa}\operatorname{erf}\left(\frac{\left(\sqrt{-{T_2}^2\varkappa}+\sqrt{-\varkappa}(n+\eta)^2\right)\sqrt{\beta}}{2(n+\eta)}\right)-e^{T_2\beta\varkappa}\right.\right. \\ &\quad \left.\left.+\operatorname{erf}\left(\frac{\left(-\sqrt{-{T_2}^2\varkappa}+\sqrt{-\varkappa}(n+\eta)^2\right)\sqrt{\beta}}{2(n+\eta)}\right)+1\right)\right)^{-1}. \end{aligned} \tag{23}$$

3.3. The Vibrational Mean Free Energy

The Helmholtz free energy is a thermodynamic potential in statistical mechanics and thermodynamics that evaluates the useful work achievable from a closed thermodynamic system with constant temperature, volume, and particle number. The Helmholtz free energy is reduced for such an equilibrium system and may be used to calculate all other thermodynamic parameters of the material. As a result, the vibrational mean free energy, through its compact form, is directly represented by

$$\begin{aligned} F(\beta) &= -\kappa T\ln Q_{vib}(\beta) \\ &= -\tfrac{1}{\beta}\left(\ln\left(\frac{1}{2\sqrt{-\varkappa\mu\beta}}\left(\left(e^{T_2\beta\varkappa}\operatorname{erf}\left(\frac{(\sqrt{-{T_2}^2\varkappa}+\sqrt{-\varkappa}(n+\eta)^2)\sqrt{\beta}}{2(n+\eta)}\right)-e^{T_2\beta\varkappa}\right.\right.\right.\right. \\ &\quad \left.\left.\left.\left.+\operatorname{erf}\left(\frac{(-\sqrt{-{T_2}^2\varkappa}+\sqrt{-\varkappa}(n+\eta)^2)\sqrt{\beta}}{2(n+\eta)}\right)+1\right)\sqrt{\pi}e^{-T_1\varkappa\beta}\right)\right)\right). \end{aligned} \tag{24}$$

3.4. The Vibrational Entropy

Entropy is an essential quantity in physics, chemistry, and biology because of its numerous applications, such as dissolution [59], fluorescence microscopy [60], adsorption [61], material creation [62], and protein activity [63]. Determining the analytical expression of entropy for diatomic molecules is still a tough proposition in science. Entropy, which may be defined and quantified in many domains other than thermodynamics, serves to assess the degree of order and disorder, or chaos. As a result, the vibrational entropy is more specifically expressed as

$$
\begin{aligned}
&S_{vib}(\beta) = \kappa \ln Q_{vib}(\beta) + kT\frac{\partial}{\partial T}\ln Q_{vib}(\beta)\\
&= \left(\kappa\left((n+\eta)\left(e^{T_2\beta\varkappa}\mathrm{erf}\left(\frac{\left(\sqrt{-{T_2}^2\varkappa}+\sqrt{-\varkappa}(n+\eta)^2\right)\sqrt{\beta}}{2(n+\eta)}\right) - e^{T_2\beta\varkappa} + \mathrm{erf}\left(\frac{\left(-\sqrt{-{T_2}^2\varkappa}+\sqrt{-\varkappa}(n+\eta)^2\right)\sqrt{\beta}}{2(n+\eta)}\right)\right.\right.\right.\\
&\left.\left.\left.+1\right)\sqrt{\pi}\ln\left(\frac{1}{2\sqrt{-\varkappa\mu\beta}}\left(\left(e^{T_2\beta\varkappa}\mathrm{erf}\left(\frac{\left(\sqrt{-{T_2}^2\varkappa}+\sqrt{-\varkappa}(n+\eta)^2\right)\sqrt{\beta}}{2(n+\eta)}\right) - e^{T_2\beta\varkappa} + \mathrm{erf}\left(\frac{\left(-\sqrt{-{T_2}^2\varkappa}+\sqrt{-\varkappa}(n+\eta)^2\right)\sqrt{\beta}}{2(n+\eta)}\right)\right.\right.\right.\right.\\
&\left.\left.\left.\left.+1\right)\sqrt{\pi}e^{-T_1\varkappa\beta}\right)\right) + \left(\tfrac{1}{2}+\varkappa(T_1-T_2)\beta\right)\sqrt{\pi}e^{T_2\beta\varkappa}(n+\eta)\mathrm{erf}\left(\frac{\left(\sqrt{-{T_2}^2\varkappa}+\sqrt{-\varkappa}(n+\eta)^2\right)\sqrt{\beta}}{2(n+\eta)}\right)\\
&-\frac{\left(-\sqrt{-{T_2}^2\varkappa}+\sqrt{-\varkappa}(n+\eta)^2\right)\sqrt{\beta}e^{-\frac{\beta\left(-\sqrt{-{T_2}^2\varkappa}+\sqrt{-\varkappa}(n+\eta)^2\right)^2}{4(n+\eta)^2}}}{2} - \frac{e^{T_2\beta\varkappa}\left(\sqrt{-{T_2}^2\varkappa}+\sqrt{-\varkappa}(n+\eta)^2\right)\sqrt{\beta}e^{-\frac{\beta\left(\sqrt{-{T_2}^2\varkappa}+\sqrt{-\varkappa}(n+\eta)^2\right)^2}{4(n+\eta)^2}}}{2}\\
&+\sqrt{\pi}\left(\left(-\tfrac{1}{2}-\varkappa(T_1-T_2)\beta\right)e^{T_2\beta\varkappa} + \left(1+\mathrm{erf}\left(\frac{\left(-\sqrt{-{T_2}^2\varkappa}+\sqrt{-\varkappa}(n+\eta)^2\right)\sqrt{\beta}}{2(n+\eta)}\right)\right)\left(T_1\varkappa\beta+\tfrac{1}{2}\right)\right)(n+\eta)\Bigg)\Bigg)\\
&\left(\sqrt{\pi}(n+\eta)\left(e^{T_2\beta\varkappa}\mathrm{erf}\left(\frac{\left(\sqrt{-{T_2}^2\varkappa}+\sqrt{-\varkappa}(n+\eta)^2\right)\sqrt{\beta}}{2(n+\eta)}\right) - e^{T_2\beta\varkappa} + \mathrm{erf}\left(\frac{\left(-\sqrt{-{T_2}^2\varkappa}+\sqrt{-\varkappa}(n+\eta)^2\right)\sqrt{\beta}}{2(n+\eta)}\right)+1\right)\right)^{-1}.
\end{aligned}
\tag{25}
$$

3.5. The Vibrational Specific Heat

The specific heat capacity of materials and components is critical in their ultimate functionality, which includes thermal storage in building elements or transitory heat flow. The associated vibrational specific heat can be described further as

$$
\begin{aligned}
&C(\beta) = -\kappa\beta^2\frac{\partial}{\partial\beta}U(\beta)\\
&= -\Bigg(\kappa\Bigg(-2e^{-\beta({\mathcal{G}_1}^2+{\mathcal{G}_2}^2-\mathcal{G}_3)}\beta\mathcal{G}_1\mathcal{G}_2\\
&-\left(\left({\mathcal{G}_1}^2+2\mathcal{G}_3\right)\beta^{\frac{3}{2}}+\frac{\sqrt{\beta}}{2}\right)\left(-1+\mathrm{erf}\left(\mathcal{G}_2\sqrt{\beta}\right)\right)\mathcal{G}_1\sqrt{\pi}e^{-\beta({\mathcal{G}_1}^2-\mathcal{G}_3)}\\
&-\mathcal{G}_2\left(\left({\mathcal{G}_2}^2-2\mathcal{G}_3\right)\beta^{\frac{3}{2}}+\frac{\sqrt{\beta}}{2}\right)\left(\mathrm{erf}\left(\mathcal{G}_1\sqrt{\beta}\right)-1\right)\sqrt{\pi}e^{-\beta({\mathcal{G}_2}^2-\mathcal{G}_3)}\\
&+\mathcal{G}_2\left(\beta^{\frac{3}{2}}{\mathcal{G}_2}^2+\frac{\sqrt{\beta}}{2}\right)\left(-1+\mathrm{erf}\left(\mathcal{G}_2\sqrt{\beta}\right)\right)\sqrt{\pi}e^{-\beta({\mathcal{G}_2}^2-2\mathcal{G}_3)}\\
&+\beta e^{-2\beta({\mathcal{G}_2}^2-\mathcal{G}_3)}{\mathcal{G}_2}^2\\
&+\mathcal{G}_1\left(\beta^{\frac{3}{2}}{\mathcal{G}_1}^2+\frac{\sqrt{\beta}}{2}\right)\left(\mathrm{erf}\left(\mathcal{G}_1\sqrt{\beta}\right)-1\right)\sqrt{\pi}e^{-\beta{\mathcal{G}_1}^2}+e^{-2\beta{\mathcal{G}_1}^2}\beta{\mathcal{G}_1}^2\\
&+\Bigg(-\frac{\mathrm{erf}\left(\mathcal{G}_1\sqrt{\beta}\right)^2}{2}\\
&+\left(e^{\mathcal{G}_3\beta}\left(\beta^2{\mathcal{G}_3}^2+1\right)\mathrm{erf}\left(\mathcal{G}_2\sqrt{\beta}\right)-\beta^2e^{\mathcal{G}_3\beta}{\mathcal{G}_3}^2-e^{\mathcal{G}_3\beta}\right.\\
&\left.+1\right)\mathrm{erf}\left(\mathcal{G}_1\sqrt{\beta}\right)-\frac{e^{2\mathcal{G}_3\beta}\mathrm{erf}\left(\mathcal{G}_2\sqrt{\beta}\right)^2}{2}\\
&+\left(-\beta^2e^{\mathcal{G}_3\beta}{\mathcal{G}_3}^2-e^{\mathcal{G}_3\beta}+e^{\mathcal{G}_3\beta}\right)\mathrm{erf}\left(\mathcal{G}_2\sqrt{\beta}\right)-\frac{e^{2\mathcal{G}_3\beta}}{2}+e^{\mathcal{G}_3\beta}-\frac{1}{2}\\
&\left.+\beta^2e^{\mathcal{G}_3\beta}{\mathcal{G}_3}^2\right)\pi\Bigg)\Bigg)\left(\pi\left(1-\mathrm{erf}\left(\mathcal{G}_1\sqrt{\beta}\right)-e^{\mathcal{G}_3\beta}\right.\right.\\
&\left.\left.+e^{\mathcal{G}_3\beta}\mathrm{erf}\left(\mathcal{G}_2\sqrt{\beta}\right)\right)^2\right)^{-1},
\end{aligned}
\tag{26}
$$

where

$$
\begin{aligned}
\mathcal{G}_1 &= \frac{\sqrt{-\varkappa{T_2}^2}}{2(n+\eta)} - \frac{(n+\eta)\sqrt{-\varkappa}}{2},\\
\mathcal{G}_2 &= \frac{\sqrt{-\varkappa{T_2}^2}}{2(n+\eta)} + \frac{(n+\eta)\sqrt{-\varkappa}}{2},\\
\mathcal{G}_3 &= \varkappa T_2.
\end{aligned}
$$

4. Discussion

In order to understand the nature of the chemical bond and the behavior of molecules for equal internuclear distance and equilibrium bond length, Figure 1 displays the variation of the modified deformed Hylleraas potential mixed directly with the improved Frost–Musulin diatomic molecular potential in terms of the internuclear separation for the different diatomic molecules. It should be noted that the value of the proposed potential rapidly reduced to a minimum at approximately certain r after which it steadily grew with increasing r. Figure 2 depicts the treatment of $1/r^2$ and the preferred approximation with various screening parameters, σ. For various values of the screening parameters, the pattern tended to accumulate asymptotically, providing a decent approximation of the system. It can be observed from Figure 3, that the energy was purely attractive in the sense that for the lower values of r_e, the energy was less appealing and less bounded, and grew vigorously as the equilibrium bond length increased.

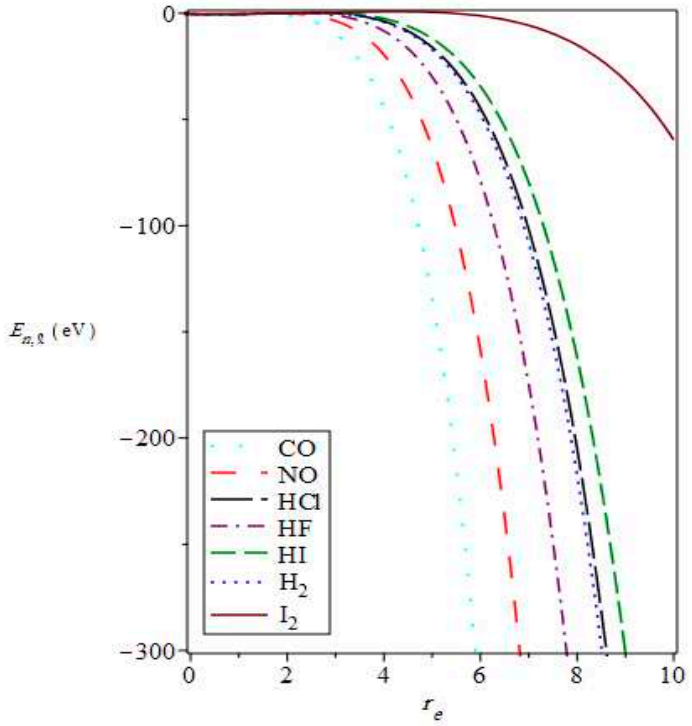

Figure 3. The function of energy spectral with regard to r_e with $(V_0, V_1, V_2, a, b) = (0.8, 0.4, 0.5, 0.6, 0.3)$ for $\sigma = 0.05$.

It is also noted that at the lower r_e, the energies for the selected diatomic molecules were almost the same, but as the equilibrium bond length increased, the energy spectra diverged significantly. Figure 4 depicts the variation of the energy eigenvalue with respect to the dissociation energy D_e, where the fluctuations of the energy spectra with D_e, illustrated a parabolic-like trend. The nonrelativistic energies increased to a peak value and later decreased as the dissociation energies increased. H_2 and HF show the monotonic drop in the energy as the dissociation energy increased, which was related to the bond length that increased as the atom's size grew, and the bond dissociation energy decreased, leading to a steady decline in the bond strength.

Figure 5 indicates the approximate energy E_{nl}, as far as the screening parameter, σ, within the proposed potential. It can be seen that as the screening parameter expanded, the energy spectra increased negatively for the selected diatomic molecules.

These diatomic substances were being evaluated for this study due to their importance in atomic, molecular, optical, and chemical physics.

In Figure 6, the behavior of the partition function was plotted as a function of the inverse temperature β. It can be concluded that there was a monotonic decrease in the partition function with increasing β for the chosen diatomic molecules.

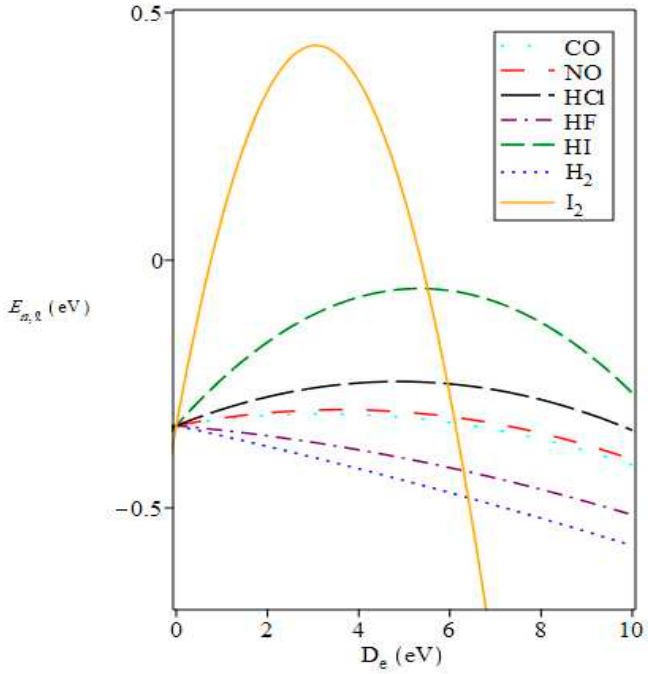

Figure 4. Contribution of the D_e^- parameters to the energy spectra with $(V_0, V_1, V_2) = (0.8, 0.4, 0.5)$, $a = 0.6$ and $b = 0.3$ for $\sigma = 0.05$.

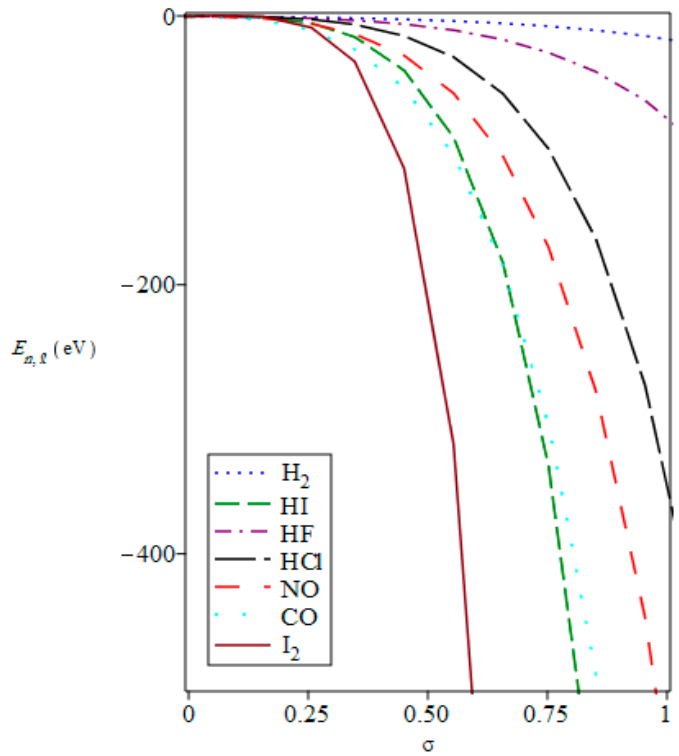

Figure 5. Effects of the screening parameter σ on the energy spectra with $(V_0, V_1, V_2, a, b) = (0.8, 0.4, 0.5, 0.6, 0.3)$.

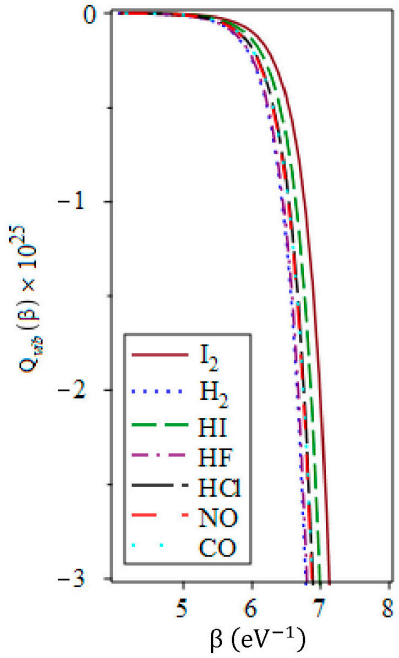

Figure 6. Variation of the partition function as a function of β for various diatomic molecules with $(V_0, V_1, V_2) = (0.8, 0.4, 0.5)$, $a = 0.6$ and $b = 0.3$ for $\sigma = 0.01$.

It can be deduced from Figure 7 that the internal energy of the diatomic molecules exhibited an exponential characteristic that decreased monotonically with increasing β.

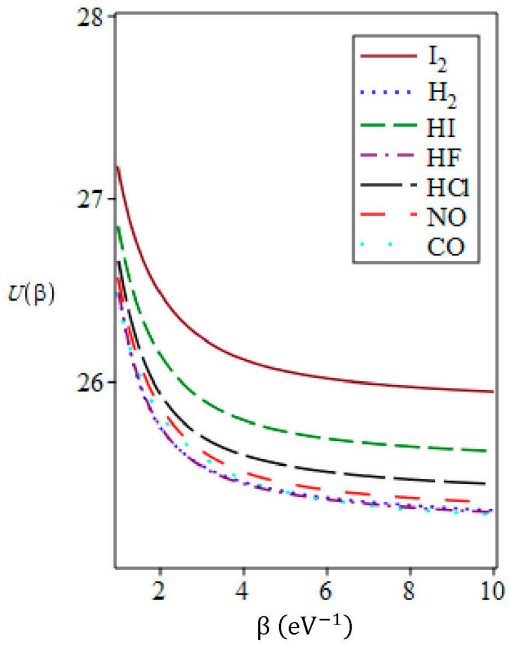

Figure 7. Behavior of the vibrational mean energy with respect to β with $(V_0, V_1, V_2) = (0.8, 0.4, 0.5)$, $a = 0.6$, $b = 0.3$, and $\sigma = 0.05$ for selected diatomic molecules.

The variations of the Helmholtz free energy F, with regard to the varied inverse temperature β, are plotted in Figure 8 for the selected diatomic molecules.

It can be seen that there is an early increase in the Helmholtz free energy as the parameter β grows and tends to converge in high β. The plots of the entropy S in terms of the inverse temperature β are displayed in Figure 9, where the curves of the entropy decayed asymptotically in the region of low temperatures.

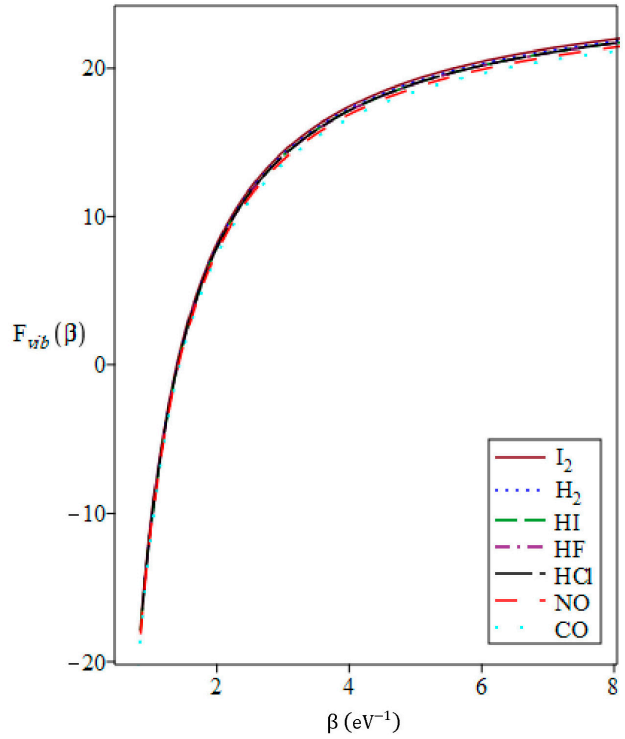

Figure 8. The contribution of β to the Helmholtz free energy with $(V_0, V_1, V_2, a, b) = (0.8, 0.4, 0.5, 0.6, 0.3)$ for $\sigma = 0.05$ for various diatomic molecules.

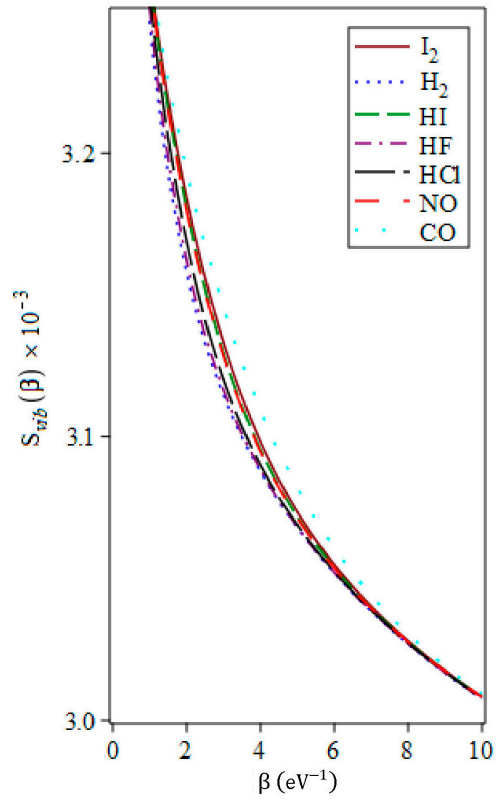

Figure 9. Effects of β on the vibrational entropy with $(V_0, V_1, V_2, a, b) = (0.8, 0.4, 0.5, 0.6, 0.3)$ for $\sigma = 0.05$ for various diatomic molecules.

Figure 10 represents the fascinating behavior of the capacity C as the inverse temperature increased.

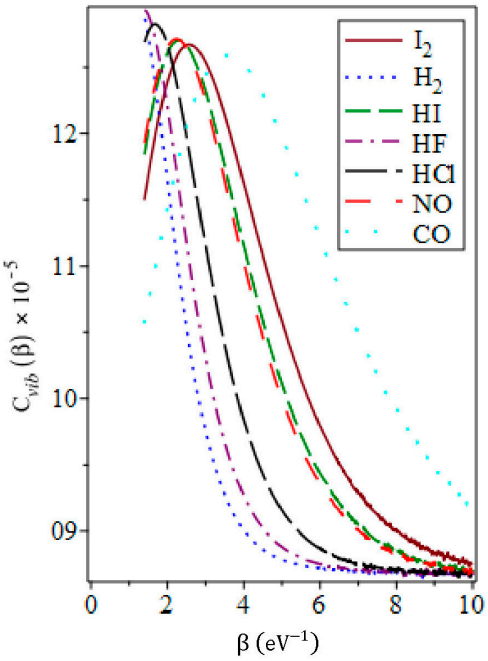

Figure 10. Variation of the vibrational specific heat with respect to β with $(V_0, V_1, V_2, a, b) = (0.8, 0.4, 0.5, 0.6, 0.3)$ for $\sigma = 0.05$ for various diatomic molecules.

In the low inverse temperature β, one can characterize an increment in the capacity C, where beyond this region, there was a descending tendency with increasing β for the selected diatomic molecules. The spectroscopic constants of the chosen diatomic molecules discussed in this research can be obtained via Table 1.

Table 1. Spectroscopic parameters of the diatomic molecules.

Molecules	r_e ()	D_e (eV)	μ (amu)
I_2	2.662	1.5556	63.45223
HI	1.6040	4.1493	1.00018
HF	0.9171	5.8856	0.95736
HCl	1.2746	4.6190	0.98010
NO	1.1508	8.0437	7.46844
CO	1.1283	11.2256	6.86067
H_2	0.7416	4.7446	0.50391

The unique cases of Equation (1) generated by choosing the proper controlling parameters might easily propose distinct interaction potential patterns. Based on this, it is possible to see that when $D_e = 0$, and $V_1 = V_2 = 0$, Equation (1) reduces to the deformed Hylleraas potential, which is a subset of the multi-parameter exponential-type potential and was first explored for diatomic molecules [64],

$$V_{DHP}(r) = \frac{V_0}{b} \cdot \frac{e^{-\sigma r} - a}{e^{-\sigma r} - 1}.$$

This form of potential, on the other hand, is a subset of the Morse potential, which has sparked a lot of attention over the years and is one of the most useful potential models for describing the interaction of two atoms in a diatomic molecule [28]. Because of its capacity to simulate the interaction of two atoms in these systems, this is considered as a persuasive model with applications in several branches of condensed matter and nuclear physics [65]. As a result, the approximate analytical solutions to the ℓ-state Schrödinger equation are derived as

$$E_{n,\ell}^{(DHP)} = \frac{1}{2\mu}\left(\left(\frac{2a\mu V_0}{\sigma^2\hbar^2 b} + \ell(\ell+1) - \left(\frac{\frac{2(1-a)\mu V_0}{\sigma^2\hbar^2 b} + \ell(2n+1) + (n+1)^2}{2(n+\ell+1)}\right)^2\right)\sigma^2\hbar^2\right). \tag{27}$$

However, when $D_e = 0$ and assigning $V_0 = V_1 = 0$, the Pöschl–Teller potential [66] is obtained as

$$V_{PTP}(r) = \frac{V_2 e^{-\sigma r}}{(1-e^{-\sigma r})^2},$$

whose energy spectra, in accordance with Equation (14), are given by

$$E_{n,\ell}^{(PTP)} = \frac{1}{2\mu}\left(\ell(\ell+1) - \left(\frac{-\ell(\ell+1)}{2n+1+2\sqrt{\left(\ell+\frac{1}{2}\right)^2+\frac{2\mu V_2}{\sigma^2\hbar^2}}} + \frac{1}{2}\left(n+\frac{1}{2}+\sqrt{\left(\ell+\frac{1}{2}\right)^2+\frac{2\mu V_2}{\sigma^2\hbar^2}}\right)^2\right)\sigma^2\hbar^2\right). \tag{28}$$

Furthermore, the results correspond well with those presented in [67] in the non-relativistic limit for the ℓ-wave case. Setting $V_2 = 0$ and $a = 0$ at $D_e = 0$ in Equation (1), yields the Hulthén potential,

$$V_{HP}(r) = \frac{(V_0 + V_1 b)e^{-\sigma r}}{b(e^{-\sigma r}-1)},$$

which is particularly essential in the atomic and molecular fields. It is a short-range potential that has been used to investigate the bound state energies of diatomic molecules [68], the optical characteristics of quantum dots [69], and other topics. Thus, given this condition, the energy eigen-spectrum may be calculated as

$$E_{n,\ell}^{(HP)} = \frac{1}{2\mu}\left(\left(\ell(\ell+1) - \left(\frac{\frac{2\mu}{\sigma^2\hbar^2}\left(\frac{V_0}{b}+V_1\right) + n(2\ell+n+2) + \ell + 1}{2(n+\ell+1)}\right)^2\right)\sigma^2\hbar^2\right).$$

In particular, the results have good agreement with those obtained in [70] as a special case. As the internuclear distance r approaches 0, it reduces to a screened coulomb potential [71,72], whereas for large values of r, it becomes a diminishing exponential potential [73]. It is demonstrated that the findings produced by this approach are compatible with the ones obtained in [71–73]. Using $D_e = 0$, as well as $V_0 = 0$, or equivalently $b \to \infty$, in Equation (1), one may produce the Eckart potential, which was established in 1930 [74] and is one of the most significant exponential-type potentials in chemical physics [75]. Applying $D_e = 0$ in addition to $V_1 = V_2 = 0$, and substituting $a = -1$ and $b = 1$, results in the Rosen–Morse potential [76], expressed as

$$V_{RMP}(r) = \frac{V_0(1+e^{-\sigma r})}{e^{-\sigma r}-1}.$$

The corresponding energy eigenvalues of this potential are calculated as

$$E_{n,\ell}^{(RMP)} = \frac{1}{2\mu}\left(\left(-\frac{2\mu V_0}{\sigma^2\hbar^2} + \ell(\ell+1) - \left(\frac{\frac{4\mu V_0}{\sigma^2\hbar^2} + n(n+2) + 1 + \ell(2n+1)}{2(n+\ell+1)}\right)^2\right)\sigma^2\hbar^2\right),$$

which agrees well with that obtained in [77]. The Frost–Musulin diatomic molecular potential has been used in a variety of fields of physics [78,79]. In the case when $V_0 = V_1 = V_2 = 0$ in Equation (1), the improved Frost–Musulin potential is obtained as

$$V_{IFMP}(r) = -\frac{D_e\Big(\big(-\sigma {r_e}^2 + r(1+\sigma r_e)\big)e^{(r_e-r)\sigma} - r\Big)}{r},$$

and the associated energy equation for this potential is provided as

$$E_{n,\ell}^{(IFMP)} = \frac{1}{2\mu}\left(\left(\frac{2\mu D_e}{\sigma^2\hbar^2}(1-(\sigma r+1)e^{\sigma r}) + \ell(\ell+1) - \left(\frac{-\frac{2D_e\mu r^2 e^{\sigma r}}{\sigma\hbar^2} + \ell(2n+1) + (n+1)^2}{2(n+\ell+1)}\right)^2\right)\sigma^2\hbar^2\right).$$

This potential model has also been shown to suit experimental data for the study of diatomic molecules [80].

5. Conclusions

Because of the intriguing characteristic of the modified deformed Hylleraas potential with the improved Frost–Musulin diatomic molecular potential (which is a more generic instance of the exponential-type ones commonly seen in many physical fields), the approximate ℓ-state solutions for the Schrödinger equation with this potential function were studied in this research utilizing the Nikiforov–Uvarov technique and the Greene–Aldrich approximation scheme. For several selected diatomic molecules, the treatment of the corresponding energy eigenvalues as a function of various potential parameters was explored. It was readily apparent that the energy spectra for the chosen diatomic molecules grew adversely when the screening parameter was raised. The partition function, as well as other thermodynamic functions such as entropy, mean free energy, and specific heat capacity, were determined in this manner. The graphs of the thermodynamic characteristics as well as β indicated that for certain diatomic molecules, there was a monotonous decline in the partition function owing to the rising B. The internal energy and the entropy dropped gradually as β boosts but Helmholtz free energy increased and tended to converge as β increased. The capacity advanced at the low inverse temperature B, with an ongoing decline as β increased. Specific samples of the potential and their analogous energy relations were determined, which were consistent with those reported in the literature. Furthermore, it is important to highlight that, to the best of our knowledge, the findings of this study have not been investigated in the prior literature, which could pave the way for additional studies in other fields of theoretical chemistry, such as mathematical chemistry, molecular mechanics, molecular dynamics, and chemical thermodynamics, to explain the geometric and electronic structures of molecular assemblies, polymers, and chemical processes.

Funding: This research received no external funding.

Data Availability Statement: The calculated and acquired data employed to support the findings of this study are included in the article and are mentioned at appropriate positions within the manuscript as references.

Acknowledgments: The author gratefully thanks the kind referees for their constructive suggestions and invaluable comments, which definitely helped to improve the readability and quality of the manuscript.

Conflicts of Interest: The author declares that there are no conflicts of interest regarding the publication of this paper.

References

1. Oluwadare, O.J.; Oyewumi, K.J. The scattering phase shifts of the Hulthén-type potential plus Yukawa potential. *Eur. Phys. J. Plus* **2016**, *131*, 295. [CrossRef]
2. Onyeaju, M.C.; Ikot, A.N.; Chukwuocha, E.O.; Obong, H.P.; Zare, S.; Hassanabadi, H. Scattering and Bound States of Klein-Gordon Particle with Hylleraas Potential Within Effective Mass Formalism. *Few Body Syst.* **2016**, *57*, 823–831. [CrossRef]
3. Onate, C.A.; Onyeaju, M.C.; Ikot, A.N. Analytical solutions of the Dirac equation under Hellmann–Frost-Musulin potential. *Ann. Phys.* **2016**, *375*, 239–250. [CrossRef]
4. Chen, C.-Y.; Sun, D.-S.; Lu, F.-L. Approximate analytical solutions of Klein-Gordon equation with Hulthén potentials for nonzero angular momentum. *Phys. Lett. A* **2007**, *370*, 219–221. [CrossRef]
5. Bayrak, O.; Soylu, A.; Boztosun, I. The relativistic treatment of spin-0 particles under the rotating Morse oscillator. *J. Math. Phys.* **2010**, *51*, 112301. [CrossRef]
6. Onate, C.A.; Onyeaju, M.C.; Ituen, E.E.; Ikot, A.N.; Ebomwonyi, O.; Okoro, J.O.; Dopamu, K.O. Eigensolutions, Shannon entropy and information energy for modified Tietz-Hua potential. *Ind. J. Phys.* **2018**, *92*, 487–493. [CrossRef]
7. Abu-Shady, M.; Abdel-Karim, T.A.; Ezz-Alarab, S.Y. Masses and thermodynamic properties of heavy mesons in the non-relativistic quark model using the Nikiforov–Uvarov method. *J. Egypt Math. Soc.* **2019**, *27*, 14. [CrossRef]
8. Khokha, E.M.; Abu-Shady, M.T.; Abdel-Karim, A. Quarkonium masses in the N-dimensional space using the analytical exact iteration method. *Int. J. Theor. Appl. Math.* **2016**, *2*, 86–92.
9. Abu-Shady, M. Heavy Quarkonia and Mesons in the Cornell Potential with Harmonic Oscillator Potential in the N-dimensional Schrödinger Equation. *Int. J. Appl. Math. Theor. Phys.* **2016**, *2*, 16–20.
10. Omugbe, E. Non-relativistic eigensolutions of molecular and heavy quarkonia interacting potentials via the Nikiforov Uvarov method. *Can J. Phys.* **2020**, *98*, 1125–1132. [CrossRef]
11. Omugbe, E. Non-relativistic Energy Spectrum of the Deng-Fan Oscillator via the WKB Approximation Method. *Asian J. Phys. Chem. Sci.* **2020**, *8*, 26–36. [CrossRef]
12. Roy, K.A. Ro-vibrational spectroscopy of molecules represented by a Tietz-Hua oscillator potential. *J. Math. Chem.* **2014**, *52*, 1405–1413. [CrossRef]
13. Diaf, A. Arbitrary l-state solutions of the Feynman propagator with the Deng-Fan molecular potential. *J. Phys. Conf. Ser.* **2015**, *574*, 012022. [CrossRef]
14. Wang, P.-Q.; Zhang, L.-H.; Jia, C.-H.; Liu, J.-Y. Equivalence of the three empirical potential energy models for diatomic molecules. *J. Mol. Spec.* **2012**, *274*, 5–8. [CrossRef]
15. Messiah, A. *Quantum Mechanics*; Dover Publication: New York, NY, USA, 2014.
16. Dong, S.-H. *Factorization Method in Quantum Mechanics*; Springer: Dordrecht, The Netherlands, 2007. [CrossRef]
17. Landau, L.D.; Lifshitz, E.M. *Quantum Mechanics, Non-Relativistic Theory*, 3rd ed.; Pergamon: New York, NY, USA, 1977.
18. Ikot, A.N.; Awoga, O.A.; Hassanabadi, H.; Maghsoodi, E. Analytical approximate solution of Schrödinger equation in D-dimensions with quadratic exponential-type potential for arbitrary l-State. *Commun. Theor. Phys.* **2014**, *61*, 457–463. [CrossRef]
19. Greene, R.L.; Aldrich, C. Variational wave functions for a screened coulomb potential. *Phys. Rev. A* **1976**, *14*, 2363–2366. [CrossRef]
20. Falaye, B.J. Arbitrary l-State Solutions of the Hyperbolical Potential by the Asymptotic Iteration Method. *Few Body Syst.* **2012**, *53*, 557–562. [CrossRef]
21. Rey, A.K. Studies on the Bound-State Spectrum of Hyperbolic Potential. *Few-Body Syst.* **2014**, *55*, 143–150. [CrossRef]
22. Liu, J.-Y.; Zhang, G.-D.; Jia, C.-S. Calculation of the interaction potential energy curve and vibrational levels for the a 3Σu + state of Li27 molecule. *Phys. Lett. A* **2013**, *377*, 1444–1447. [CrossRef]
23. Jia, C.-S.; Chen, T.; He, S. Bound state solutions of the Klein–Gordon equation with the improved expression of the Manning-Rosen potential energy model. *Phys. Lett. A* **2013**, *37*, 682–686. [CrossRef]
24. Roy, B.; Roychoudhury, R. The shifted 1/N expansion and the energy eigenvalues of the Hulthén potential for $l \neq 0$. *J. Phys. A Math. Gen.* **1987**, *20*, 3051–3055. [CrossRef]
25. Nikiforov, A.F.; Uvarov, V.B. *Functions of Mathematical Physics*; Birkhäuser: Basel, Switzerland, 1988. [CrossRef]
26. Roshanzamir, M. The Information-Theoretic Treatment of Spinless Particles with the Assorted Diatomic Molecular Potential. *Adv. High Energy Phys.* **2022**, *2022*, 6621156. [CrossRef]
27. Tezcan, C.; Sever, R. A General Approach for the Exact Solution of the Schrödinger Equation. *Int. J. Theor. Phys.* **2009**, *48*, 337–350. [CrossRef]
28. Bayrak, O.; Boztosun, I.; Çiftci, H. Exact analytical solutions to the Kratzer potential by the asymptotic iteration method. *Int. J. Quantum Chem.* **2006**, *107*, 540–544. [CrossRef]
29. Stahlhofen, A.; Bleuler, K. An algebraic form of the factorization method. *Nuov. Cim. B* **1989**, *104*, 447–465. [CrossRef]
30. Edelstein, R.M.; Govinder, K.S.; Mahomed, F.M. Solution of ordinary differential equations via nonlocal transformations. *J. Phys. A Math. Gen.* **2001**, *34*, 1141–1152. [CrossRef]
31. Falaye, B.J.; Ikhdair, S.M.; Hamzavi, M. Formula Method for Bound State Problems. *Few Body Syst.* **2015**, *56*, 63–78. [CrossRef]
32. Ikot, A.N.; Hassanabadi, H.; Maghsoodi, E.; Zarrinkamar, S. D-Dimensional Dirac Equation for Energy-Dependent Pseudoharmonic and Mie-type Potentials via SUSYQM. *Commun. Theor. Phys.* **2014**, *61*, 436–446. [CrossRef]
33. Fa-Lin, L.; Chang-Yuan, C.; Dong-Sheng, S. Bound states of Klein–Gordon equation for double ring-shaped oscillator scalar and vector potentials. *Chin. Phys.* **2005**, *14*, 463–467. [CrossRef]

34. Dong, S.-H.; Ma, Z.-Q. Exact solutions to the Schrödinger equation for the potential $V(r) = ar^2 + br^{-4} + cr^{-6}$ in two dimensions. *J. Phys. A Math. Gen.* **1998**, *31*, 9855–9859. [CrossRef]
35. Roshanzamir-Nikou, M.; Goudarzi, H. The Laplace transform approach for a Dirac isotonic oscillator with a tensor potential in D-dimensions. *Phys. Scr.* **2013**, *89*, 015001. [CrossRef]
36. Roshanzamir-Nikou, M.; Goudarzi, H. Pauli isotonic oscillator with an anomalous magnetic moment in the presence of the Aharonov–Bohm effect: Laplace transform approach. *Theor. Math. Phys.* **2016**, *186*, 286–293. [CrossRef]
37. Tang, H.-M.; Liang, G.-C.; Zhang, L.-H.; Zhao, F.; Jia, C.-S. Diatomic molecule energies of the modified Rosen−Morse potential energy model. *Can. J. Chem.* **2014**, *92*, 341–345. [CrossRef]
38. Hu, X.-T.; Zhang, L.-H.; Jia, C.-S. D-dimensional energies for cesium and sodium dimers. *Can. J. Chem.* **2014**, *92*, 386–391. [CrossRef]
39. Qiang, W.-C.; Dong, S.-H. Proper quantization rule. *EPL (Europhys. Lett.)* **2010**, *89*, 10003. [CrossRef]
40. Oluwadare, O.J.; Oyewumi, K.J. Scattering state solutions of the Duffin-Kemmer-Petiau equation with the Varshni potential model. *Eur. Phys. J. A* **2017**, *53*, 29. [CrossRef]
41. Jing, J.; Zhang, Y.-F.; Wang, K.; Long, Z.-W.; Dong, S.-H. On the time-dependent Aharonov-Bohm effect. *Phys. Lett. B* **2017**, *774*, 87–90. [CrossRef]
42. Yeşiltaş, Ö.; Şimşek, M.; Sever, R.; Tezcan, C. Exponential Type Complex and Non-Hermitian Potentials in PT-Symmetric Quantum Mechanics. *Phys. Scr.* **2003**, *67*, 472–475. [CrossRef]
43. Onyenegecha, C.P.; Onate, C.A.; Echendu, O.K.; Ibe, A.A.; Hassanabadi, H. Erratum to: Solutions of Schrodinger equation for the modified Mobius square plus Kratzer potential. *Eur. Phys. J. Plus* **2020**, *135*, 382. [CrossRef]
44. Hatami, N.; Naji, J.; Pananch, M. Analytical solutions of the Klein-Gordon equation for the deformed generalized Deng-Fan potential plus deformed Eckart potential. *Eur. Phys. J. Plus* **2019**, *134*, 90. [CrossRef]
45. Hassanabadi, H.; Maghsoodi, E.; Zarrinkamar, S.; Rahimov, H. An approximate solution of the Dirac equation for hyperbolic scalar and vector potentials and a Coulomb tensor interaction by SUSYQM. *Mod. Phys. Lett. A* **2011**, *26*, 2703–2718. [CrossRef]
46. Dong, S.-H.; Cruz-Irisson, M. Energy spectrum for a modified Rosen-Morse potential solved by proper quantization rule and its thermodynamic properties. *J. Math. Chem.* **2012**, *50*, 881–892. [CrossRef]
47. Ikot, A.N.; Akpan, I.O. Bound State Solutions of the Schrödinger Equation for a More General Woods-Saxon Potential with Arbitrary l-state. *Chin. Phys. Lett.* **2012**, *29*, 090302. [CrossRef]
48. Peña, J.J.; García-Martínez, J.; García-Ravelo, J.; Morales, J. Bound state solutions of D-dimensional schrödinger equation with exponential-type potentials. *Int. J. Quantum Chem.* **2014**, *115*, 158–164. [CrossRef]
49. Suparmi, A.; Cari, C.; Pratiwi, B.N. Thermodynamics properties study of diatomic molecules with q-deformed modified Poschl-Teller plus Manning Rosen non-central potential in D dimensions using SUSYQM approach. *J. Phys. Conf. Ser.* **2016**, *710*, 012026. [CrossRef]
50. Ikhdair, S.M.; Sever, R. Polynomial solutions of the Mie-type potential in the D-dimensional Schrödinger equation. *J. Mol. Struct. Theochem* **2008**, *855*, 13–17. [CrossRef]
51. Oyewumi, K.J. Analytical Solutions of the Kratzer-Fues Potential in an Arbitrary Number of Dimensions. *Found. Phys. Lett.* **2005**, *18*, 75–84. [CrossRef]
52. Gradshteyn, I.S.; Ryzhik, I.M. *Table of Integrals, Series and Products*, 7th ed.; Elsevier: Amsterdam, The Netherlands; Academic Press: Cambridge, MA, USA, 2007; ISBN 978-0-12-373637-6/978-0-12-373637-4.
53. Gensterblum, Y.; Busch, A.; Krooss, B.M. Molecular concept and experimental evidence of competitive adsorption of H_2O, CO_2 and CH_4 on organic material. *Fuel* **2014**, *115*, 581–588. [CrossRef]
54. Skouteris, D.; Calderini, D.; Barone, V. Methods for calculating partition functions of molecules involving large amplitude and/or anharmonic motions. *J. Chem. Theory Comput.* **2016**, *12*, 1011–1018. [CrossRef]
55. Ikot, A.N.; Chukwuocha, E.O.; Onyeaju, M.C.; Onate, C.A.; Ita, B.I.; Udoh, M.E. Thermodynamic properties of diatomic molecules with general molecular potential. *Pramana J. Phys.* **2018**, *90*, 22. [CrossRef]
56. Njegic, B.; Gordon, M.S. Exploring the effect of anharmonicity of molecular vibrations on thermodynamic properties. *J. Chem. Phys.* **2006**, *125*, 224102. [CrossRef] [PubMed]
57. Song, X.-Q.; Wang, C.-W.; Jia, C.-S. Thermodynamic properties for the sodium dimer. *Chem. Phys. Lett.* **2017**, *673*, 50–55. [CrossRef]
58. Ebeling, W.; Sokolov, I.M. *Statistical Thermodynamics and Stochastic Theory of Nonequilibrium Systems*; World Scientific: Singapore, 2005. [CrossRef]
59. Song, W.; Martsinovich, N.; Hecklabd, W.M.; Lackinger, M. Thermodynamics of halogen bonded monolayer self-assembly at the liquid–solid interface. *Chem. Commun.* **2014**, *50*, 13465–13468. [CrossRef]
60. Yahiatène, I.; Hennig, S.; Huser, T. Optical fluctuation microscopy based on calculating local entropy values. *Chem. Phys. Lett.* **2013**, *587*, 1–6. [CrossRef]
61. Ammendola, P.; Raganati, F.; Chirone, R. CO_2 adsorption on a fine activated carbon in a sound assisted fluidized bed: Thermodynamics and kinetics. *Chem. Eng. J.* **2017**, *322*, 302–313. [CrossRef]
62. Moses, S.A.; Covey, J.P.; Miecnikowski, M.T.; Yan, B.; Gadway, B.; Ye, J.; Jin, D.S. Creation of a low-entropy quantum gas of polar molecules in an optical lattice. *Science* **2015**, *350*, 659–662. [CrossRef]
63. Tzeng, S.R.; Kalodimos, C.G. Protein activity regulation by conformational entropy. *Nature* **2012**, *488*, 236–240. [CrossRef]

64. Varshni, Y.P. Comparative Study of Potential Energy Functions for Diatomic Molecules. *Rev. Mod. Phys.* **1957**, *29*, 664–682. [CrossRef]
65. Ejere, A.I.I.; Ebomwonyi, O. Hylleraas potential quantum well in Cu_2ZnSnS_4 quaternary semiconductor alloy in the presence of magnetic field. *Mater. Res. Express* **2019**, *6*, 096411. [CrossRef]
66. Pöschl, G.; Teller, E. Bemerkungen zur Quantenmechanik des anharmonischen Oszillators. *Z. Physik* **1933**, *83*, 143–151. [CrossRef]
67. Akcay, H.; Sever, R. Analytical solutions of Schrödinger equation for the diatomic molecular potentials with any angular momentum. *J. Math. Chem.* **2012**, *50*, 1973–1987. [CrossRef]
68. Aydoğdu, O.; Arda, A.; Sever, R. Scattering of a spinless particle by an asymmetric Hulthén potential within the effective mass formalism. *J. Math. Phys.* **2012**, *53*, 102111. [CrossRef]
69. Onyeaju, M.C.; Idiodi, J.O.A.; Ikot, A.N.; Solaimani, M.; Hassanabadi, H. Linear and Nonlinear Optical Properties in Spherical Quantum Dots: Generalized Hulthén Potential. *Few Body Syst.* **2016**, *57*, 793–805. [CrossRef]
70. Taskin, F.; Kocak, G. Approximate solutions of Schrödinger equation for Eckart potential with centrifugal term. *Chin. Phys. B* **2010**, *19*, 090314. [CrossRef]
71. Liverts, E.Z.; Drukarev, E.G.; Krivec, R.; Mandelzweig, V.B. Analytic presentation of a solution of the Schrödinger equation. *Few Body Syst.* **2008**, *44*, 367–370. [CrossRef]
72. Edet, C.O.; Okorie, U.S.; Ngiangia, A.T.; Ikot, A.N. Bound state solutions of the Schrodinger equation for the modified Kratzer potential plus screened Coulomb potential. *Indian J. Phys.* **2020**, *94*, 425–433. [CrossRef]
73. Bayrak, O.; Boztosun, I. Bound state solutions of the Hulthén potential by using the asymptotic iteration method. *Phys. Scr.* **2007**, *76*, 92. [CrossRef]
74. Eckart, C. The Penetration of a Potential Barrier by Electrons. *Phys. Rev.* **1930**, *35*, 1303–1309. [CrossRef]
75. Cimas, A.; Aschi, M.; Barrientos, C.; Rayón, V.M.; Sordo, J.A.; Largo, A. Computational study on the kinetics of the reaction of N(4S) with CH_2F. *Chem. Phys. Lett.* **2003**, *374*, 594–600. [CrossRef]
76. Jia, C.-S.; Dai, J.-W.; Zhang, L.-H.; Liu, J.-Y.; Zhang, G.-D. Molecular spinless energies of the modified Rosen–Morse potential energy model in higher spatial dimensions. *Chem. Phys. Lett.* **2015**, *619*, 54–60. [CrossRef]
77. Ikot, A.N.; Awoga, O.A.; Antia, A.D. Bound state solutions of D-dimensional Schrödinger equation with Eckart potential plus modified deformed Hylleraas potential. *Chin. Phys. B* **2013**, *22*, 020304. [CrossRef]
78. Frost, A.A.; Musulin, B. Semiempirical Potential Energy Functions. I. The H_2 and H^{2+} Diatomic Molecules. *J. Chem. Phys.* **1954**, *22*, 1017. [CrossRef]
79. Jia, C.-S.; Diao, Y.-F.; Liu, X.-J.; Wang, P.-Q.; Liu, J.-Y.; Zhang, G.-D. Equivalence of the Wei potential model and Tietz potential model for diatomic molecules. *J. Chem. Phys.* **2012**, *137*, 014101. [CrossRef] [PubMed]
80. Adepoju, A.G.; Eweh, E.J. Approximate and analytical bound state solutions of the Frost–Musulin potential. *Can. J. Phys.* **2014**, *92*, 18–21. [CrossRef]